JPRS-JST-89-020
13 OCTOBER 1989

FOREIGN
BROADCAST
INFORMATION
SERVICE

JPRS Report

Science & Technology

Japan

ATOMIC ENERGY SOCIETY
1989 ANNUAL MEETING

JPRS-JST-89-020
13 OCTOBER 1989

SCIENCE & TECHNOLOGY

JAPAN

ATOMIC ENERGY SOCIETY

1989 ANNUAL MEETING

43063045 Osaka NIHON GENSHIRYOKU GAKUKAI 1989 NENKAI [1989 ANNUAL MEETING OF THE ATOMIC ENERGY SOCIETY OF JAPAN] in Japanese 4-6 Apr 89 pp 1-285

[Selected abstracts of papers presented at the 1989 Annual Meeting of the Atomic Energy Society of Japan held 4-6 Apr 89 in Osaka]

CONTENTS

High Density Implosion of Plastic Shell Targets by Gekko X II Green Laser

43063045a Osaka NIHON GENSHIRYOKU GAKUKAI 1989 NENKAI in Japanese 4-6 Apr 89
p 21

[Abstract A21 by M. Yamanaka, K. Mima, N. Mayanaga, H. Azechi, M. Takagi, A. Nishiguchi, P. A. Norrays, H. Nishimura, H. Nakaishi, M. Saito, O. Maekawa, Y. Setsuhara, Y.-W. Chen, M. Unemoto, T. Yamashita, Y. Shimada,[a] M. Katayama,[b] T. Jitsuno, M. Nakatsuka, K. Yoshida, K. Kobayashi,[a] I. Kimura,[b] C. Yamanaka,[c] and S. Nakai, Laser Laboratory, Osaka University. [a]Nuclear Reactor Laboratory, Kyoto University. [b]Faculty of Engineering, Kyoto University. [c]Comprehensive Laser Laboratory.]

[Text] We irradiated plastic, hollow shell targets with Gekko X II green laser beams in a spherically symmetric pattern and generated high density implosions (the world's highest density), achieving a density over 600 times the initial solid density (total density of 1.1 g/cm^3, heavy water density of 0.16 g/cm^3).

It is necessary to improve the spherical symmetry of implosion to obtain high density implosions. To reach a high density, we improved (a) the uniformity of laser irradiation and (b) the uniformity of plastic shell targets. To achieve (a), the energy balance of the Gekko X II green laser beams (12 beams) was controlled within ±3 percent. Moreover, random phase plates (RPP) were used to make each beam's intensity distribution uniform. To achieve (b), high quality pellets [made of] CD, CDTH and CDTSi, whose shell thicknesses were uniform within one percent, were used.

To measure the density-radius product ($\rho_D R$) of the densely compressed core, the secondary reaction method was used when $\rho_D R < 0.005$ -- 0.010 g/cm^2, the proton knock-on method when $\rho_D R < 0.030$ g/cm^2, and neutron emission from Si when $\rho_D R > 0.030$ g/cm^2. The density ρ_D was derived from the value of $\rho_D R$ measured earlier using the residual mass obtained from measuring the mass extrusion rate, $\dot{m}$.

In Fig. 1, we present the dependence of the fuel ρR (i.e., $\rho_D R$) value on the shell thickness. Filled squares, circles, and triangles refer to plastic shells 900 μm, 700 μm, and 500 μm in diameter, respectively; R denotes the data obtained using the RPP's. The maximum value of $\rho_D R$ for ordinary laser beams when RPP's were not used was about 0.030 g/cm^2, which corresponds to a compression of about 100 fold. When RRP's were used, however, $\rho_D R$ = 0.22 g/cm^2 was achieved, indicating a compression of more than 600 fold. The peak of $\rho_D R$ was located at a shell thickness of 9 to 10 μm when irradiated with RPP's. We estimate that this represents the optimum results in implosion efficiency, preheating, and probably even in hydrodynamical instability. The open triangles in Fig. 1, which match experimental data well, are examples of one-dimensional fluid simulation calculations that determine the thermal conduction of electrons by solving the Fokker-Planck equation.

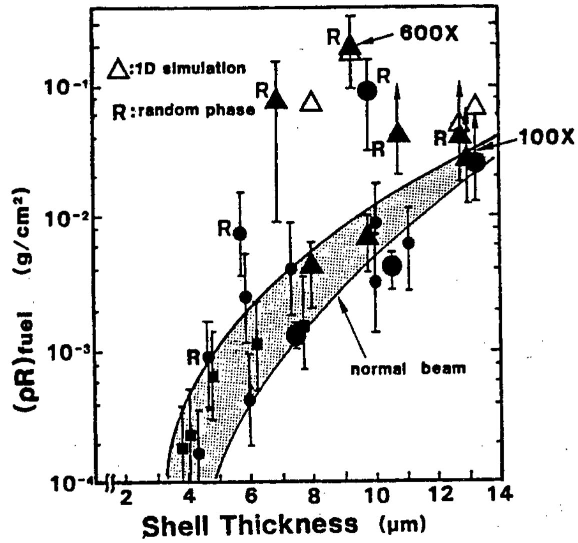

Figure 1. Dependence of $\rho_D R$ on plastic shell thickness.

At the meeting, we will compare experimental details to simulation results.

Development of Simplified Impact Analysis Code for Nuclear Fuel Shipping Casks

43063045b Osaka NIHON GENSHIRYOKU GAKUKAI 1989 NENKAI in Japanese 4-6 Apr 89
p 39

[Abstract A39 by T. Ikushima, Japan Atomic Energy Research Institute]

[Text] 1. Introduction

We have been developing a code system to analyze the thermal and structural safety of nuclear fuel shipping casks. We recognized the need for a simplified analytic code that could perform sensitivity and other analyses for safety evaluation rapidly, and we decided to add the CASKETSS code system. As part of this system, we have developed CRUSH, a code to analyze a cask's collision by dropping; FINCRUSH, a code to analyze the collision of cooling fins on the outside of a cask; and PUNCTURE, a code to analyze the puncturing of a cask.

2. Simplified Analysis Codes

CRUSH: CRUSH uses the UDM (Uniaxial Displacement Method),[2] which was developed from the VDM (Volumetric Displacement Method),[1] as shown in Fig. 1. In the UDM, materials serving as shock absorbers are considered to be a collection of one-dimensional rods that do not interact with each other. The effect of structural materials (such as covers) covering the shock absorbers is evaluated by using springs equivalent to their rigidity or end constraint factors.

3. Verification Calculation

Figure 1. Method to calculate collision acceleration.

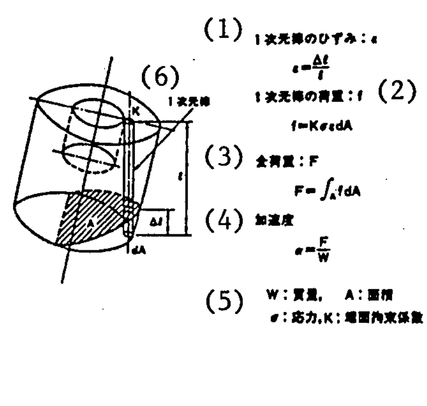

Key to Fig. 1:
(1) Strain on one-dimensional rod
(2) Load on one-dimensional rod
(3) Total load
(4) Acceleration
(5) W=mass, A=area, sigma=strain, K=end constraint factor
(6) One-dimensional rod

Figure 2. Effect of collision angle on acceleration.

Key to Fig. 2:
(1) Collision angle
(2) Experiment
(3) Calculation
(4) Acceleration

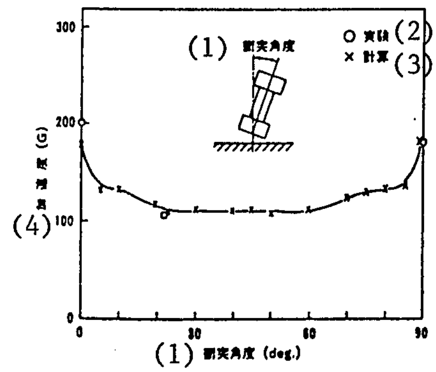

Figure 3. Effect of collision angle on displacement.

Key to Fig. 3:
(1) Collision angle
(2) Experiment
(3) Calculation
(4) Displacement

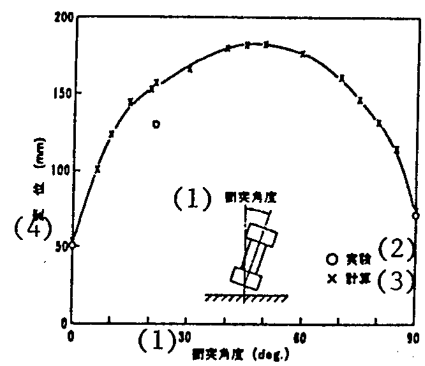

Results obtained from CRUSH were compared to experimental results from the United States to verify the appropriateness of the calculated results. In the experiment, one-quarter scale models of NUPAC-125B shipping casks (for TMI-2 debris) were dropped from a height of 9 m. Results of this experiment and our calculated results are compared in Figs. 2 and 3. These figures present acceleration and displacement as functions of the collision angle. The figures demonstrate that the values calculated from the simplified analysis code, CRUSH, are mostly appropriate when compared to experimental values.

References

1. B. J. Donham, Proceedings of Seminar (Vienna), International Atomic Energy Agency, pp. 509--523 (1971).
2. Ohashi, Asada, et al., Mitsubishi Heavy Industries Report, Vol. 17, No. 3 (1980).

Measurement of Void Reactivity Worth of Experimental Control Rod Hole in VHTRC-1 Core

43063045c Osaka NIHON GENSHIRYOKU GAKUKAI 1989 NENKAI in Japanese 4-6 Apr 89 p 91

[Abstract C1 by F. Akino, T. Yamane, M. Takeuchi, and Y. Kaneko, Japan Atomic Energy Research Institute]

[Text] There are three insertion holes, for two control rods and an absorber from the post-shutdown system, in the control rod column of the high temperature test reactor (HTTR). Using the PNS method, the void reactivity worth of the simulated control rod insertion holes in the VHTRC-1 core was measured to evaluate the neutron streaming effect due to these holes' void.

Experiment

Four BF_3 detectors, each 1/4 inch in diameter, were inserted into the VHTRC-1 core loaded with 278 fuel rods (4 percent enriched uranium). The PNS target was placed at the back center of the 1/2 assembly on the fixed side. Voids (10.2 cm in diameter and 240 cm long) were created by removing graphite rods from the simulated control rod insertion holes at the center column, as shown in Fig. 1. The void reactivity worth was measured using the PNS method with one, two or three voids. The reactivity worth was calculated using the modified King-Simmons reactivity formula[1] that corrected for variations in the neutron generation time.

Calculation

Details of the fuel column grid pattern were taken into consideration, and a constant for 24 groups (11 groups of fast neutrons and 13 groups of thermal neutrons) was calculated with a 61-group grid using the collision probabilities determined from SRAC.[2] Another 24-group constant was determined for the center column using the same procedure. The diffusion coefficient was evaluated using the following two models:

Homogeneous model

$$D_{homo} = 1/3\Sigma_{tr} \quad \cdots\cdots (1)$$

Inhomogeneous model (Benoist model)

$$D_k = (\sum_i \varphi_i \cdot \sum_j \frac{P_{ijk}}{\Sigma_{tr,j}})/3\sum_i \varphi_i \quad \cdots\cdots (2)$$

($D_{k=r}$ = diffusion coefficient in the radial direction; $D_{k=z}$ = diffusion coefficient in the axial direction) The ratio of the diffusion coefficients obtained from Eqs. (1) and (2) is shown in Fig. 2. A triangular mesh was used to represent the hexagonal core shape, and the core calculation was carried out using a 24-group, three-dimensional diffusion code, CITATION. D_{homo} from Eq. (1) or D_r and D_z from Eq. (2) were used as the diffusion coefficient of the center column to calculate K_{eff} with and without voids and to obtain the corresponding reactivity worth. Calculated and measured values of the reactivity worth are listed in Table 1.

Table 1. Void reactivity worth of simulated control rod insertion holes in the center column.

Number of voids in center column	Measured values (*)	Calculated values (*) D_{homo}	D(Benoist model)
1	0.77 ± 0.02	0.3998	0.7826
2	1.53 ± 0.03	0.8823	1.628
3	2.33 ± 0.04	1.443	2.488

[* Original illegible--translator]

Conclusion

The values of void reactivity worth calculated by considering the inhomogeneity of diffusion coefficients agreed with the measured values within 7 percent. Also, we found that these calculated values of the reactivity worth of the simulated control rods were affected by about 3 percent when calculated based on a system where the insertion holes were taken as voids and the inhomogeneity of diffusion coefficients was ignored.

Figure 1. Fuel rods loaded in the core of VHTRC-1.

Key to Fig. 1:
(1) Insertion holes for simulated control rods
(2) Center column
(3) Fuel rods
(4) Safety rods
(5) Control rods
(6) BF_3 detectors
(7) 1/2 assembly on the fixed side

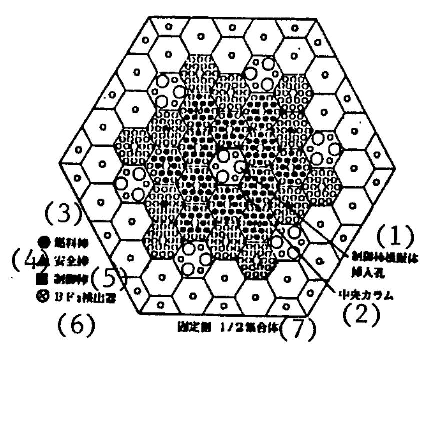

Figure 2. Difference between Benoist's coefficients and $D_{homo} = 1/3\ \Sigma_{tr}$.

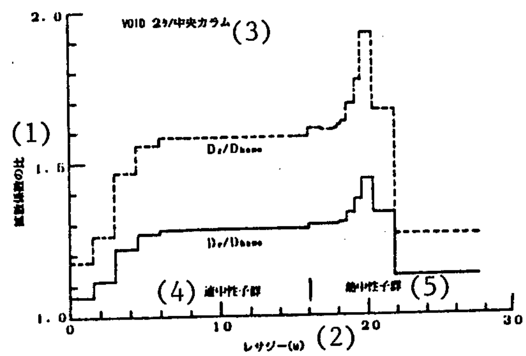

Key to Fig. 2:

(1) Ratio of the diffusion coefficients
(2) Lethargy (u)
(3) Two voids in the center column
(4) Fast neutron group
(5) Thermal neutron group

References

1. Akino et al., Abstract C45, 1988 Fall Annual Meeting of the Atomic Energy Society of Japan.
2. K. Tsuchihashi et al., Japan Atomic Energy Research Institute [Report Number] 1302 (1986).

Measurement of MEU [Medium Enriched Uranium] Fuel Element Characteristics in JRR-2

43063045d Osaka NIHON GENSHIRYOKU GAKUKAI 1989 NENKAI in Japanese 4-6 Apr 89 p 101

[Abstract C11 by Y. Matsui, H. Kikuchi, T. Sato, T. Kiuchi, M. Nakano, D. Nemoto, T. Yamada, I. Aoyama, J. Tsunoda, and Y. Futamura, Japan Atomic Energy Research Institute]

[Text] Introduction

JRR-2 is a heavy water reactor consisting of 24 fuel elements units and six control rods in its core. Is has a thermal output of 10 MW and runs in a 21-day cycle; it operates continuously for 12 days and then shuts down for 9 days for maintenance such as fuel replacement and inspection.

As part of the RERTR program, it was decided to switch the JRR-2 fuel from a mixture of square and cylindrical rods of highly enriched uranium (93 percent U-235) to cylindrical rods of medium enriched uranium (45 percent U-23). As a result, the characteristics of the medium enriched core were measured for about two months, from the end of November 1987 to the end of January 1988.

We describe these characteristics measurements in this report.

2. Characteristics Measurements and Results

In a criticality test, fuel rods were inserted in succession, starting from the A ring. The first criticality of the MEU core was achieved at the eleventh rod (U-235 mass of 2223 g), as expected. The results are shown in Fig. 1.

Reactivity measurements were carried out on the effects of the temperature, pump, heavy-water dump, and thermal shielding light water reflector. The results were almost equivalent to the case of the HEU core.

The fast neutron flux was approximately equal to that for the HEU core, but the thermal neutron flux was somewhat lower than the expected value.

While the fuel reactivity of the A ring was slightly lower than that for the HEU core, the reactivities of the B, C, and D rings hardly changed.

The control rod corrections for JRR-2 are determined every year by the positive core period (PP) method. This time, we also used the control-rod drop method (integration method), since this is the starting MEU core. The control rod corrections determined from the PP method were at about the same level as those for the HEU core. The control-rod drop method was not as accurate as the PP method. We believe that this deficiency occurred because some of the BF_3 counters used were not included. After correcting for this possibility, we obtained results similar to that from the PP method.

Upon comparing the saturation value and variation of the Xe-135 poisoning effect after a reactor shutdown to those of the HEU core, we found that the reactivity [of the MEU core] was reduced slightly because its average thermal neutron flux was lower than that for the HEU core.

3. Conclusion

The results of our characteristics measurement are listed in Table 1. According to the table, we observed no significant differences between the characteristics of the MEU core and those of the HEU core. Thus, we confirmed that JRR-2 successfully switched from the HEU core to the MEU core without reducing its performance and without operational problems in using the new fuel.

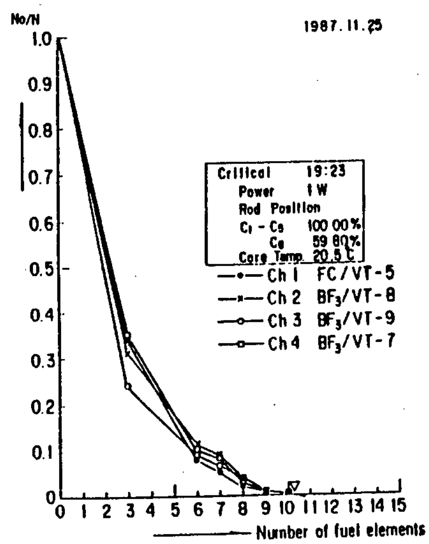

Fig. 1 Critical Curves

Table 1. Measured characteristics of JRR-2 (MEU and HEU core).

Item	Unit	MEU core values	HEU core values
Critical mass (U-235)	g	2223	2184
Excess reactivity	%Δk/k	17.3	15
Total control-rod worth	%Δk/k	32.9	35
Moderator temperature coefficient (17°C)	%Δk/k/°C	$-1.9 \times 10^{-*}$	$-2.0 \times 10^{-*}$
Average thermal neutron flux in core (fuel rod *)	a/cm^2-sec	$5 \times 10^{1*}$	$8 \times 10^{1*}$

[* Original illegible--translator]

Collisional Processes in Laser Isotope Separation III Crossed Beam Technique Using Laser-Produced Ion Beam to Measure Charge Transfer Cross Sections

43063045e Osaka NIHON GENSHIRYOKU GAKUKAI 1989 NENKAI in Japanese 4-6 Apr 89 p 174

[Abstract J54 by T. Sudo, M. Hashida, S. Sakabe, M. Kosaka, A. Tada, Y. Izawa, T. Yamanaka, S. Nakai, and C. Yamanaka[a], Laser Laboratory, Osaka University. [a]Comprehensive Laser Laboratory.]

[Text] Atomic collisions in a metal vapor during the recovery of isotope ions excited selectively represent one of the reasons for the low concentration in laser isotope separation. Important collisional processes are (1) charge transfer collisions, (2) excitation transfer collisions, and (3) ionization by electron impact. In particular, an important cause for the reduced of concentration as atomic density increases is the charge transfer collisions between [neutral] atoms and ions. While the ^{235}U ions ionized by laser are polarized by the collecting electric field, they pass through an atomic beam of ^{238}U and capture electrons through charge transfer collisions, thus allowing ^{238}U ions to be collected and the concentration [of ^{235}U] to be reduced. Hence, it is important to study experimentally the charge transfer collision cross sections to choose the vapor density in the designing a laser isotope separation apparatus. Up to now, not enough was known about the charge transfer cross sections of metallic atoms, except for alkali atoms. We built a crossed-beam collision apparatus for a laser-produced ion beam and an atomic vapor beam generated by electron-gun heating in order to measure such collision cross sections.

The atomic beam was formed by collimating metal vapor. Since we had to heat metals with high melting points, such as gadolinium, to more than 2000°C to have a sufficient vapor pressure, and since a crucible corroded easily at such high temperatures, we chose vaporization by electron beam heating, which provided sufficient yet localized heating. Also, since we had to generate an abundant, low-velocity ion beam with little energy spread, we used photoionization by an ArF laser [to generate the ion beam]. The collision vacuum chamber was divided into two parts, a vapor generating part and a collision part, each of which was pumped to 10^{-7} torr using a turbomolecular pump.

Two atomic beams were generated, one of which was irradiated with light focussed by an F/10 lens to generate ions by photoionization.

The ions generated were polarized and focussed using electrodes and lenses; the ion beam was guided to collide with the other atomic beam. The amount of ions was measured by an ion collector and the atomic beam density was determined by a thick-film monitor installed at the top. Ions generated by charge transfer were led to a secondary electron multiplier by lenses and a curved electrode. Coincidence measurements of collision parameters are necessary to determine cross sections for charge transfer collisions that occur during one laser pulse.

A data processing system based on the CAMAC System was used to measure the energy change of the pulsed excimer laser used to generate the ion beam, the time variation of vapor generated by the electron gun, ion beam signal intensity, and the charge transfer signal intensity. Thus, we are now able to measure charge transfer collision cross sections of metals with high precision. We will measure charge transfer collision cross sections of many metals in the future using this apparatus. We will describe the structure and characteristics of this apparatus at the meeting.

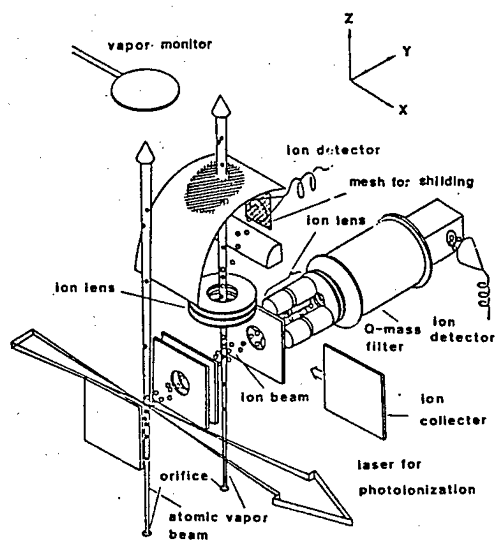

Figure 1. Measurement of charge transfer collision cross sections by crossing atomic and ion beams.

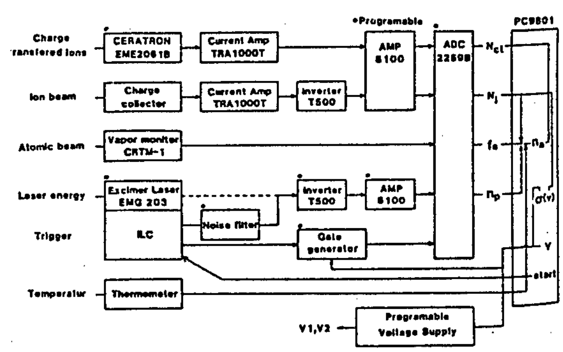

Figure 2. Data collection system for crossed-beam collision experiment.

Fast Breeder Reactor Spent Fuel Reprocessing Hot Test U/Pu Partition Process with Lactic Acid

43063045f Osaka NIHON GENSHIRYOKU GAKUKAI 1989 NENKAI in Japanese 4-6 Apr 89 p 255

[Abstract L29 by T. Yasu, O. Tayoda, S. Ohtake, A. Todokoro, and Y. Kishimoto, Power Reactor and Nuclear Fuel Development Corporation.]

1. Introduction

While the Purex method partitions U and Pu by reducing Pu, it requires re-oxidation to refine Pu. To simplify the partitioning process, we separated U and Pu by forming a lactic acid complex of Pu while keeping it in a quadrivalent state. We report our results here.

2. Trial Method

In our experiment, we performed parameter tests by experimenting in beakers, continuous partitioning tests based on these parameter tests, and tests to separate Pu and lactic acid. In the beaker experiments, the partition coefficients of U and Pu in 30 percent TBP [tributyl phosphate] were measured while the lactic acid concentration was varied between 0.3 M and 2.0 M and the nitric acid concentration between 0.5 M and 4.0 M The continuous partitioning tests were conducted using a mixer-settler according to the flow chart shown in Fig. 1, which was based on the partition coefficients obtained from the beaker experiments. In the Pu-lactic acid separation tests, the separability of Pu and lactic acid was measured by using a mixer-settler in a mixture of lactic acid and nitric acid, whose concentrations were kept at 3 to 4 N.

3. Test Results

We confirmed that lactic acid does separate U and Pu well, as described below.

(1) As a result of the parameter beaker tests, we found that the partition coefficient of Pu^{4+} decreased as the lactic acid concentration increased, while the coefficient increased as the nitric acid concentration rose. On the other hand, the partition coefficient of U varied with the nitric acid concentration in the same way as Pu^{4+} did but the dependence of the coefficient on the lactic acid concentration was opposite to that of Pu^{4+}.

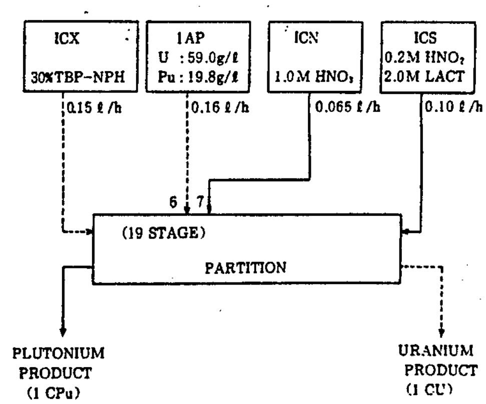

Figure 1. Lactic acid partition flow chart.

(2) Based on the beaker experiments, the optimum concentrations of lactic and nitric acids which reduced the partition coefficient of Pu^{4+} while maintaining that of U were taken to be 2.0 M and 0.2 M, [respectively].

(3) As a result of the continuous partitioning tests, we obtained $DF_U = 4.5 \times 10^2$ and $DF_{Pu} = 1.8 \times 10^5$. (See Table 1.)

Table 1. Results of partitioning by lactic acid.

Puプロダクト中 U濃度 (g/ℓ) (1)	DF_U	Uプロダクト中の Pu濃度 (g/ℓ) (2)	DF_{Pu}
0.12	4.5×10^2	$<0.05\times10^{-3}$	1.8×10^5

$$DF_U = \frac{Pu_{Pu\ product} : U_{Pu\ product}}{Pu_{FEED}\ U_{FEED}}$$

$$DF_{Pu} = \frac{U_{U\ product}\ Pu_{U\ product}}{U_{FEED}\ Pu_{FEED}}$$

Key to Table 1:
(1) Concentration of U in the Pu product
(2) Concentration of Pu in the U product

(4) In separating Pu and lactic acid, we were able to reduce the lactic acid concentration in the Pu solution to 7×10^{-3} M by solvent extraction, while keeping the nitric acid concentration in the mixture of lactic acid and nitric acid to 3 to 4 N.

4. Future Tasks

(1) Confirmation of the effects of depleted materials.
(2) Rationalization of the waste liquid processing method.

Experimental Analysis of Control Rod Worth of KUCA Core

43063046a Osaka NIHON GENSHIRYOKU GAKUKAI 1989 NENKAI in Japanese 4-6 Apr 89 p 94

[Abstract C4 by T. Kugo,[a] K. Sengoku,[a] T. Takeda,[a] K. Kobayashi,[b] Y. Ogawa,[c] K. Kanda,[d] S. Shiroya,[d] and Other Members of the Joint University Team for High [Efficiency] Converter Research. [a]Faculty of Engineering, Osaka University. [b]Faculty of Engineering, Kyoto University. [c]Faculty of Science and Engineering, Kinki University. [d]Reactor Center, Kyoto University.]

[Text] Introduction

The control rod worth of the solid moderation mount of the Kyoto University Critical Assembly (KUCA) is reported to be negative[1] based on a diffusion calculation. To verify the method used in evaluating the control rod worth, the control rod worth and the gold (Au) reaction rate distribution near the control rod channels were measured while the absorber rods were fully inserted or completely removed. We report the results of an analysis based on transport and diffusion calculations.

Calculations

Three-dimensional system calculations were performed in four groups using a diffusion calculation code, CITATION, and the transport SN calculation code we developed, Tritac. Thus calculated, the control rod worth and the gold reaction rate distribution were compared with experimental values. The control rod worth was determined as follows:

$$\text{Control Rod Worth} = (1/k_{eff})_{CR(In)} - (1/k_{eff})_{CR(Out)}.$$

Results

The control rod worth values are listed in Table 1. Values obtained by transport calculation agreed with the experimental values within about 10 percent, while diffusion calculation led to negative values. The gold reaction rates when the absorber rods were fully inserted and completely removed are plotted in Figs. 1 and 2. Calculated values, using both the diffusion and transport methods, took a shape similar to that of the experimental values when the control rods were inserted. When the rods were removed, however, only the transport calculation values nearly reproduced the shape of the experimental values inside the control rod channels, while the diffusion calculation values exhibited a shape different from that of the experimental values. The neutron flux distribution in the XZ plane that passed the center of the control rod channels in the four groups (below 0.68 eV), when the absorber rods were completely removed, is shown in Figs. 3 and 4. From these figures, one can see that neutrons leak out of the reactor core through the control rod channels, which became empty when the absorbers were removed in the diffusion calculation. We found that the control rod worth became negative because the neutron leak through the area free of absorber rods was exaggerated in the diffusion calculation.

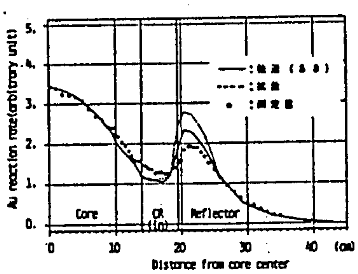

Fig. 1. Gold reaction rate distribution with absorber rods fully inserted.

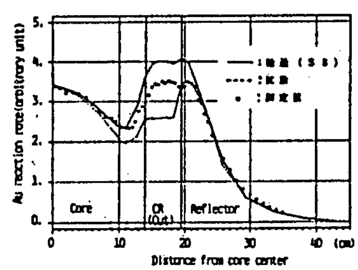

Fig. 2. Gold reaction rate distribution with absorber rods completely removed.

Legend for Figs. 1 and 2:
Solid curve : Transport calculation (S8)
Dotted curve : Diffusion calculation
Filled circles: Experimental values

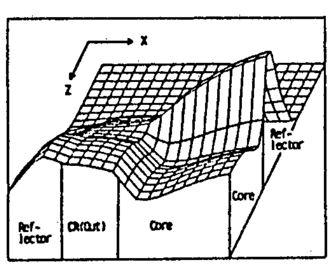

Fig. 3. Thermal neutron flux distribution in the XZ plane based on transport calculation (S8) with the absorber rods completely removed.

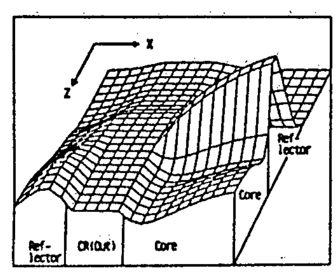

Fig. 4. Thermal neutron flux distribution on the XZ plane based on diffusion calculation (S8) with the absorber rods completely removed.

Table 1. Control rod worth (%dk/kk').

Diffusion	-0.299	Transport (S4)	0.554
Experiment	0.622	Transport (S8)	0.569

This research was part of the KUCA Joint Utilization Experiment conducted by the Joint University Team for High Converter Research.

Reference

1. Kimura et al., Abstract D30, 1987 Fall Annual Meeting [of the Atomic Energy Society of Japan].

Measurement and Analysis of Decay Heat of Spent Fuel from Joyo
(2) Measurement and Analysis of Decay Heat of Spent Fuel

43063046b Osaka NIHON GENSHIRYOKU GAKUKAI 1989 NENKAI in Japanese 4-6 Apr 89
p 116

[Abstract C26 by Y. Arii, H. Nagasaki,[a] Y. Okimoto, M. Tashiro, and M. Mizoo, Power Reactor and Nuclear Fuel Development Corporation (Oarai). [a]Nuclear Power System.]

[Text] 1. Introduction

We report the measurement of decay heat of spent fuel from Joyo using a device described earlier, and its analysis using the decay heat evaluation code, FPGS.

2. Method of Analysis

The decay heat was calculated as follows. The actual data produced by the operation monitoring code for Joyo, MAGI (for a three-dimensional Hex-Z diffusion calculation), were used as input to the FPGS code to analyze the output of the spent fuel assembly, its irradiation history and fuel composition. The neutron spectrum at the irradiation location was determined using the CITATION code (for a two-dimensional R-Z diffusion calculation) and then used as input to the FPGS code. Spent fuel was cooled for one cycle (about 70 days) on a fuel storage rack inside the reactor. The heat generated during this period was assumed to be about 10 percent of the heat generated in the reactor core.

3. Experimental Results

The decay heat measured using 34 fuel assemblies from the reactor core is shown in Fig. 1. The results with the highest decay heat (PFD153) measured from the core fuel are plotted in Fig. 2. PFD153 was loaded into the third row of the reactor core, had an assembly output of 1.47 MW, and had its average degree of burn-up of 64,000 MWd/t. Its measured decay heat was about

690 MW, while the calculated value at the same time was about 710 MW, resulting in a calculated to the experimental value ratio (C/E) of 1.04. (Contributions to the decay heat from fission products and structural materials are shown in Fig. 2, the former contributing about 80 percent.) The C/E values of other fuel assemblies also range between 0.83 and 1.10, demonstrating relatively good agreement.

We studied the (C/E) trend using the data obtained so far. As is shown in Fig. 3, C/E tends to decrease as time elapsed after normal operations were completed. This indicates a trend that the calculated values decrease relative to the measured values when the cooling period is extended. Additional trends in C/E and other factors will be examined and discussed [at the conference].

4. Conclusion

Very few examples of a comprehensive evaluation of decay heat of spent fuel from a fast [neutron] reactor are available in the world. Our experiment confirmed the effectiveness of our decay heat measurement device (effectiveness of the experimental method). Our results can be used in the logical design of a decay heat removal system for a fast neutron reactor by using the results to improve the precision of decay heat evaluation.

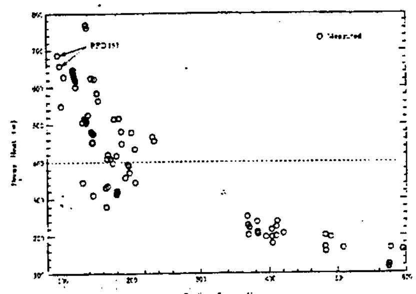

Fig.1 Decay Heat of JOYO Spent Fuel

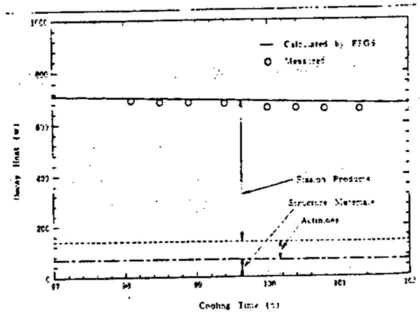

Fig.2 Decay Heat of PFD153

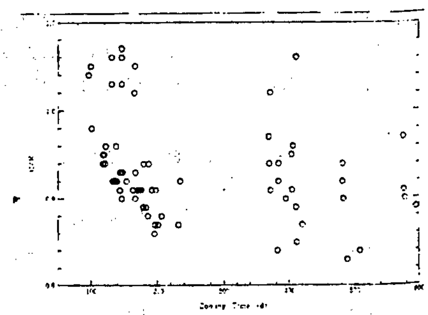

Fig.3 Cooling Time Dependence of C/E

Design Study of High Breeding Metallic Fuel Fast Reactor (IV)
--Feasibility Study on Tube-in-Shell Type Fuel Assembly (2)

43063046c Osaka NIHON GENSHIRYOKU GAKUKAI 1989 NENKAI in Japanese 4-6 Apr 89
p 179

[Abstract D29 by T. Ishii,[a] T. Sato,[a] K. Sako, H. Takano, and T. Hiraoka,
Japan Atomic Energy Research Institute. [a]MAPI.]

1. Objective

We reported at the last meeting[1] a study of the structural concept and basic feasibility of an FP gas purge, tube-in-shell metal fuel assembly. In this work, we report on a study of systematic evaluation procedures for this fuel assembly's integrity and problems associated with fuel fabrication.

2. Evaluation System for the Integrity of Fuel Assembly

The tube-in-shell fuel assembly itself requires an integrity similar to that of conventional fuel elements. Hence, an important issue is the integrity of the cooling pipes themselves, the welded parts between the cooling pipes and the lower tie plate, the cooling pipe parts that pass through the upper tie plate, the shell pipes themselves, and of the joints between the shell pipes and the upper and lower tie plates. The evaluation procedures are very different from those used for ordinary metal fuels; the procedures are complicated because the overall behavior of the fuel assembly must be evaluated. An evaluation flow chart has been developed by examining the relationships between individual phenomena and their influence on items to be evaluated for integrity.

Fig. 1. Fabrication of the fuel assembly using the sliding method.

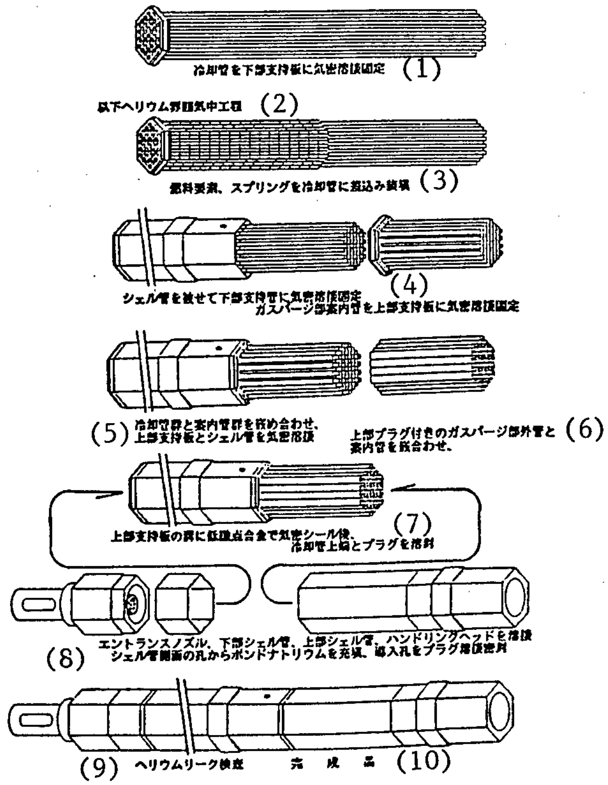

Key to Fig. 1:
(1) Cooling pipes are airtightly welded to the bottom tie plate.
(2) All of the following processing is done in a helium atmosphere.
(3) Fuel elements and springs are inserted into cooling pipes.
(4) Pipes are covered by a shell and then welded airtightly to lower support tubes. Gas purge guiding tubes are welded airtightly to the upper tie plate.
(5) Cooling pipes and guiding tubes are fitted together and the upper tie plate is welded airtightly to the shell.
(6) Gas purge outer tubes with upper plugs are fitted to the guiding tubes.
(7) These fitted tubes are sealed airtightly into the grooves in the upper tie plate by a low melting-point alloy, and the top end of the cooling pipes and plugs are melted and sealed.
(8) The entrance nozzle, lower shell, upper shell, and handling head are welded; bonding sodium is filled through a hole on the side of the shells; and the filling holes are sealed by welding plugs.
(9) The product is checked for helium leaks.
(10) Finished product.

3. Fabrication Procedure for the Fuel Assembly

This fuel assembly is fundamentally different in structure from that of a conventional pin-type fuel assembly. Figure 1 illustrates the procedure for fabricating a fuel assembly using the sliding method. Because of sodium bonding, major processing of the assembly is done vertically.

4. Fabrication of Fuel Elements (Separated Type)

In view of the heat removal characteristics and irradiation deformation characteristics, we used separated-type fuel elements formed by combining hollow cylindrical pellet[2] elements of Pu-U-Zr alloy and hollow hexagonal elements of U-Zr alloy.

Since it is difficult to fabricate hollow pellet elements by injection casting, we studied manufacturing alternatives by comparing various methods, such as press formation, extrusion, and powder metallurgy.

[References]

1. Preprint F2, Fall Annual Meeting of 1988.
2. Presented at this annual meeting.

Numerical Simulation of Dose Distribution Characteristics Around the Tokai Nuclear Site in an Emergency

43063046d Osaka NIHON GENSHIRYOKU GAKUKAI 1989 NENKAI in Japanese 4-6 Apr 89
p 2

[Abstract G2 by M. Chino, Japan Atomic Energy Research Institute.]

1. Introduction

In order to effectively carry out disaster prevention in an area adjacent [to a reactor site] in an emergency such as a reactor accident, it is important to fully understand beforehand the characteristics of atmospheric diffusion and dose distribution peculiar to the site. In this study, the wind pattern of the neighborhood of the Tokai nuclear site was investigated, and a numerical analysis of the dose distribution was carried out using the wind pattern and an emergency environmental dose data prediction system, SPEEDI, developed by the Japan Atomic Energy Research Institute [JAERI].

2. Analysis of Meteorological Data

According to the data collected from JAERI's 40-m high meteorological observation tower, the prevailing wind comes from the northeast in spring to fall, caused by high pressures located in the north, and from the northwest in the winter, due to high pressures located in the west. These winds continue for a long time, accounting for about 30 percent of the wind [observed]. Typical cases of wind direction changing greatly for a short period are caused by passing low pressures or by the sea-land wind common in the Tokai area in the summer. Dose distribution and diffusion were analyzed by choosing the northeast wind as the pattern associated with a steady wind direction and long but narrow dose distribution, and the sea-land wind as the pattern associated with a widely fluctuating wind direction and wide angular distribution.

3. Numerical Evaluation

In our numerical analysis, we assumed the [radiation] release altitude to be 150 m, the amount of rare gases released to be 1 Ci, and release into the environment to last 15 hours after a shutdown. In the case of the land-sea breeze, the beginning of the release was assumed to be the time when the wind changes from land to from the sea, since this was likely to result in the widest angular distribution. In the case of the northeast wind, the wind speed was taken to be the annual average value of the northeast wind, 4 m/s; the atmospheric stability condition was assumed to be neutral, as is mostly the case; and the wind direction was assumed to remain northeast steadily. Typical observation data on the land-sea breeze cycle, which became apparent in the field tests JAERI conducted in Tokai, were used as meteorological data for the land-sea breeze. Our model to evaluate atmospheric diffusion and dose numerically solves an advection-diffusion equation that includes the effects of time and spatial variations in concentration and dose distributions and topography.

4. Results of Analysis

Figure 1 compares external exposure dose distribution patterns over the land when radiation is released for one hour during a steady state [of the wind] and during a land-sea breeze direction change. In both cases, the contour lines represent 3×10^{-6} mrem. In a steady-state release, the distribution became a so-called Gauss plume. Meanwhile, the distribution associated with the changing wind direction of the land-sea breeze represented an exposure due to the plume, which extended south due to brief north winds appearing during the changing time, sliding inland due to the breeze from the sea. The shape of the plume resembled a fan open to about 90°. The accumulated exposure did not amount to much in distant places where the concentration was low because the exposure was temporary, resulting in a radius of fan-shaped plume substantially shorter than that of the steady-state distribution. However, the area affected by the shifting breeze pattern was about 1.5 times larger than the area affected by the steady-state exposure if all radiation were to be released in one hour during the shifting breeze.

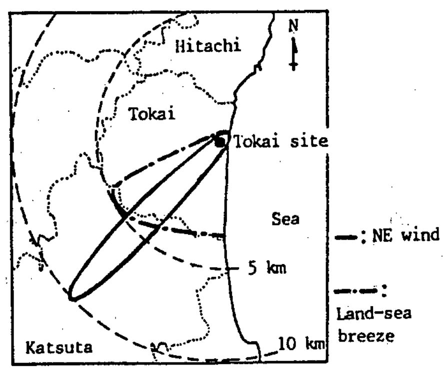

Fig. 1. Comparison of external exposure dose patterns generated by the release during steady-state and land-sea breeze shift (for one hour).

Post-Irradiation Examination of Fugen MOX Fuel Assembly Outline of the PIE

43063046e Osaka NIHON GENSHIRYOKU GAKUKAI 1989 NENKAI in Japanese 4-6 Apr 89
p 72

[Abstract H20 by K. Asahi, K. Domoto, T. Kajiyama, K. Tobita, F. Miyamoto,[a] and Y. Okuda,[a] Power Reactor Construction and Operations Headquarters, Power Reactor and Nuclear Fuel Development Corporation. [a] Fugen Power Plant.]

1. Introduction

Fugen is the world's first thermal neutron reactor to use MOX [mixed oxide] fuel in full scale, and it has steadily operated and provided data for the use of MOX fuel assemblies. As of December 1988, a total of 385 MOX fuel assemblies have been loaded into Fugen.

In order to verify the reliability of Fugen's MOX fuel assemblies under ordinary operating conditions and to confirm the appropriateness of its fuel design, JAERI is conducting post-irradiation tests [on the fuel assemblies] using its practical fuel testing facility. Some additional tests are being conducted at the irradiated fuel testing facility of the Power Reactor and Nuclear Fuel Development Corporation [PNC].

2. Tests Conducted

Post-irradiation tests started in September 1983 using one MOX fuel assembly each from the first loading and the third replacement. The post-irradiation test procedure is illustrated in Fig. 1. Each of the two fuel assemblies was irradiated for five cycles, during which operational data, such as the power output of each, were collected. The average degree of burn-up of the fuel assemblies was 13.6 GWd/t for the initial load assembly and 18.1 GWd/t for the third replacement assembly.

The post-irradiation tests included tests on fuel assembly, nondestructive tests of fuel rods, destructive tests of fuel rods, and tests of structural components of fuel assembly. The results of these tests will be presented in subsequent reports. The irradiated fuel testing facility of the PNC conducted fuel rod destruction tests to supplement data.

3. Results

(1) The irradiation behavior of the MOX fuel assemblies in Fugen confirmed the predicted irradiation behavior. Their integrity was also confirmed; there was no abnormal deformation or damage.

(2) No differences in the irradiation behavior of MOX fuel assemblies and UO_2 fuel assemblies were observed when the data collected in our experiment and BWR fuel data were compared.

(3) From (1) and (2) above, the appropriateness of the Fugen fuel design process has been confirmed.

These results indicate that the fuel fabrication technique, quality control, fuel transportation, fuel management at the reactor site, and the reactor operation and management technique are appropriate and reliable.

Details of these test and evaluation results are presented in subsequent reports.

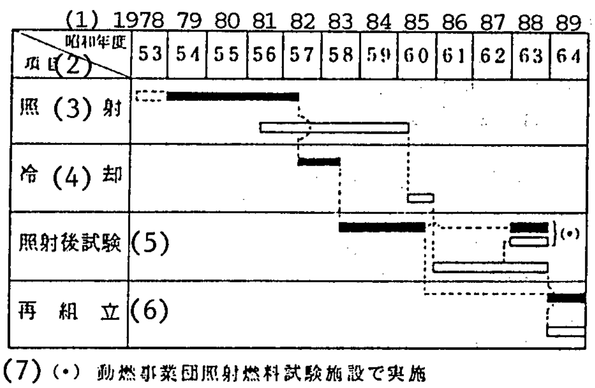

Fig. 1. Post-irradiation test procedure.

Key to Fig. 1:
(1) Year
(2) Item
(3) Irradiation
(4) Cooling
(5) Post-irradiation tests
(6) Re-assembly
(7) Conducted at the irradiated fuel test facility of PNC.

Study of Np Separation Process in Fuel Reprocessing Plants

43063046f Osaka NIHON GENSHIRYOKU GAKUKAI 1989 NENKAI in Japanese 4-6 Apr 89 p 256

[Abstract L30 by G. Uchiyama, S. Hotoku, T. Kihara, S. Fujine, and M. Maeda, Japan Atomic Energy Research Institute]

1. Introduction

Neptunium exhibits a complicated extraction behavior because it exists in the form of ions with several valence values in the Purex process solution, eventually dispersing itself into several waste solutions. The authors are developing a single cycle process that will effectively and logically separate and retrieve Np by reprocessing it, which is important to TRU [transuranium] waste management. In an earlier paper,[1] we reported a study of the butyl aldehyde reducing separation process based on distribution equilibrium data and batch extraction data. We have continued this project and now report data collected on the reducing reaction rate in the aqueous phase of (hexavalent) Np by butyl aldehyde and the results of a continuous counter-current separation experiment, conducted using a multistage minimixer-settler.

2. Experimental Method

(1) Experiment to collect reducing reaction rate data--The valence of Np(6) was adjusted by electrolysis. Samples of (hexavalent) Np and nitric acid adjusted to proper concentrations were placed in a 1-cm square quartz cell. After the liquid reached a constant temperature, we added a fixed amount of butyl aldehyde and measured the amount of (pentavalent) Np produced using a spectrophotometer (Hitachi U3410).

(2) Continuous counter-current separation experiment--This experiment was conducted on a uranium-neptunium mixture using a 16-stage minimixer-settler (made by Sonaru [phonetic translation] of France, Sirano type, 6 ml mixer section and 17 ml settler section), 8 stages for the joint extraction of U and Np, and 8 stages for their separation. The major experimental parameters were: feed liquid (3.1 N of nitric acid, 200 g/l of U, 78 mg/l of Np, and 87.5 ml/hr of flow rate), extraction solvent (30 percent TBP/nDD, and 150 ml/hr of flow rate), Np separation liquid (3.1 N of nitric acid, 3.0 percent butyl aldehyde, and 32.5 ml/hr of flow rate).

3. Experimental Results

(1) Reducing reaction rate data--In a 50°C aqueous solution with 3 N nitric acid, where an excessive amount of butyl aldehyde compared to Np existed, the reducing reaction of (hexavalent) Np proceeded rapidly and an almost complete reduction occurred in about 10 minutes. The effect of temperature on the reduction rate of (hexavalent) Np is shown in Fig. 1 as an Arrhenius plot. The following equation represents the reducing reaction rate of Np in a 3 N nitric acid aqueous solution:

$$dNp(6)/dt = 5.5 \times 10^4 \exp(-7.2 \times 10^3/1.9872t) \times Np(6).$$

(2) Continuous counter-current separation--The time needed for both U and Np concentrations in a U product liquid to reach a steady state was found to be almost the same, about three hours.

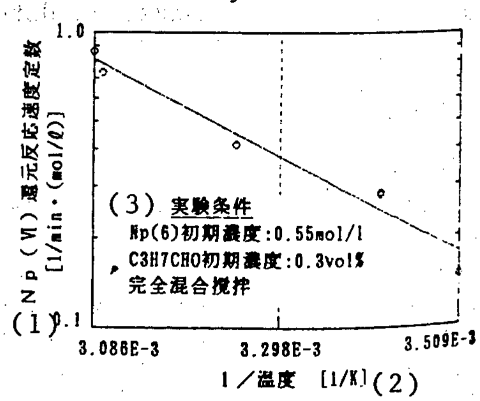

Fig. 1. The temperature dependence of Np(VI) reducing reaction rate.

Key to Fig. 1:
(1) Np (VI) reducing reaction rate constant
(2) 1/temperature
(3) Experimental conditions: initial concentration of Np(6) was 0.55 mol/l; initial concentration of C_3H_7CHO was 0.3 percent volume; samples were completely mixed by stirring

Also, approximately 90 percent of the Np extracted in the organic phase was reverse extracted by the 8-stage separation process. From these results, we conclude that butyl aldehyde is an effective reducing agent for (hexavalent) Np.

Reference

1. Abstract K-37, 1988 Fall Annual Meeting.

Removal of Np in the Reconversion Process of UF_6 by Ammonium Diuranate

43063046g Osaka NIHON GENSHIRYOKU GAKUKAI 1989 NENKAI in Japanese 4-6 Apr 89 p 257

[Abstract L31 by K. Nishimura, T. Onoue, S. Nakabayashi,[a] H. Tanaka, S. Tanaka, and Y. Fujikawa,[a] Mitsubishi Metal Corporation. [a]Mitsubishi Nuclear Fuel Company]

1. Introduction

Uranium recovered by reprocessing spent fuel contains traces of transuranium elements such as neptunium. Since this recovered uranium may be reused as nuclear fuel, it is important to establish methods to remove these elements when the recovered uranium is reconverted. We studied a method to remove Np using a chelate resin in a waste liquid produced when UF_6 is reconverted to UO_2 using the ADU [ammonium diuranate] method.

2. Testing Method

Test liquid--The process waste liquid produced in a reconversion was reprocessed by waste liquid processing (scavenging-precipitation processing) and a tracer solution of ^{237}Np was added until the ^{237}Np concentration reached 10^{-3}--10^{-7} microCi/cm^3 to prepare the test liquid. The tracer solution was prepared by first solidifying a 3N-HNO_3 acidic ^{237}Np solution by evaporation, dissolving this solid in an HF aqueous solution to obtain an HF acidic ^{237}Np solution, adding NH_3 water to achieve a pH exceeding 10, and finally filtering with a membrane filter.

Testing apparatus and testing method--Ten ml of a chelate resin was placed in a 10-mm diameter teflon column and the test liquid was passed through this column for 10 to 100 hours at a space velocity (S.V.) of $10h^{-1}$. Uniselec UR-3100 was used as the chelate resin. The ^{237}Np concentration in the test liquid processed by this chelate resin was determined using alpha spectrometry. In determining this concentration, separation preprocessing was carried out by solvent extraction using TBP-xylene. When the ^{237}Np concentration was low, further concentration preprocessing was applied by coprecipitation with $FeCl_3$.

3. Test Results

In Table 1, we show the dependence of the ^{237}Np removal rate on its concentration when the test liquid, which was prepared by adding ^{237}Np to an actual waste liquid to reach a concentration of 10^{-3} to 10^{-6} microCi/cm^3, was processed for 10 hours using the chelate resin. In Table 2, we also present the time dependence of the ^{237}Np removal rate when the test liquid, spiked with ^{237}Np to a concentration of the order of 10^{-7} microCi/cm^3, was processed for 100 hours. In both cases, the rate with which ^{237}Np was removed from the actual waste liquid produced in a reconversion processing was about 99 percent when the ^{237}Np concentration ranged from 10^{-3} to 10^{-7} microCi/cm^3.

Table 1. ^{237}Np removal rate by chelate resin (concentration dependence).

(1) 試験液の ^{237}Np濃度 (μCi/cm^3)	(2) 処理液の ^{237}Np濃度 (μCi/cm^3)	(3) ^{237}Np除去率 (%)
4.3×10^{-3}	3.8×10^{-5}	99.1
3.2×10^{-4}	2.7×10^{-5}	99.2
9.3×10^{-5}	4.9×10^{-8}	99.5

(4) 通液時間： 10 h

Key to Table 1:
(1) ^{237}Np concentration in the test liquid
(2) ^{237}Np concentration in the processed liquid
(3) ^{237}Np removal rate
(4) Liquid passing time: 10 hours

Table 2. ^{237}Np removal rate by chelate resin (time dependence).

(1) 通　液　時　間 (h)	(2) 処理液の ^{237}Np濃度 (μCi/cm^3)	(3) ^{237}Np除去率 (%)
0 ～ 50	5.4×10^{-9}	99.4
50 ～ 75	1.2×10^{-8}	98.6
75 ～ 100	9.9×10^{-9}	98.8

(4) 試験液の^{237}Np 濃度： 8.4×10^{-7} μCi/cm^3

Key to Table 2:
(1) Passing time
(2) ^{237}Np concentration in the processed liquid
(3) ^{237}Np removal rate
(4) ^{237}Np concentration in the test liquid: 8.4×10^{-7} microCi/cm^3

4. Conclusion

We found that the decontamination factor (DF) using a chelate resin to remove Np, which was contained in a process waste liquid produced during the reconversion of recovered uranium with the ADU method, was about 100 when the ^{237}Np concentration in the waste liquid ranged from 10^{-3} to 10^{-7} microCi/cm^3.

\- END -

/10

22161
45
NTIS
ATTN: PROCESS 103
5285 PORT ROYAL RD
SPRINGFIELD, VA 22161

Foreign Broadcast Information Service (FBIS) and Joint Publications Research Service (JPRS) publications contain political, economic, military, and sociological news, commentary, and other information, as well as scientific and technical data and reports. All information has been obtained from foreign radio and television broadcasts, news agency transmissions, newspapers, books, and periodicals. Items generally are processed from the first or best available source; it should not be inferred that they have been disseminated only in the medium, in the language, or to the area indicated. Items from foreign language sources are translated; those from English-language sources are transcribed, with personal and place names rendered in accordance with FBIS transliteration style.

Headlines, editorial reports, and material enclosed in brackets [] are supplied by FBIS/JPRS. Processing indicators such as [Text] or [Excerpts] in the first line of each item indicate how the information was processed from the original. Unfamiliar names rendered phonetically are enclosed in parentheses. Words or names preceded by a question mark and enclosed in parentheses were not clear from the original source but have been supplied as appropriate to the context. Other unattributed parenthetical notes within the body of an item originate with the source. Times within items are as given by the source. Passages in boldface or italics are as published.

SUBSCRIPTION/PROCUREMENT INFORMATION

The FBIS DAILY REPORT contains current news and information and is published Monday through Friday in eight volumes: China, East Europe, Soviet Union, East Asia, Near East & South Asia, Sub-Saharan Africa, Latin America, and West Europe. Supplements to the DAILY REPORTs may also be available periodically and will be distributed to regular DAILY REPORT subscribers. JPRS publications, which include approximately 50 regional, worldwide, and topical reports, generally contain less time-sensitive information and are published periodically.

Current DAILY REPORTs and JPRS publications are listed in *Government Reports Announcements* issued semimonthly by the National Technical Information Service (NTIS), 5285 Port Royal Road, Springfield, Virginia 22161 and the *Monthly Catalog of U.S. Government Publications* issued by the Superintendent of Documents, U.S. Government Printing Office, Washington, D.C. 20402.

The public may subscribe to either hardcover or microfiche versions of the DAILY REPORTs and JPRS publications through NTIS at the above address or by calling (703) 487-4630. Subscription rates will be provided by NTIS upon request. Subscriptions are available outside the United States from NTIS or appointed foreign dealers. New subscribers should expect a 30-day delay in receipt of the first issue.

U.S. Government offices may obtain subscriptions to the DAILY REPORTs or JPRS publications (hardcover or microfiche) at no charge through their sponsoring organizations. For additional information or assistance, call FBIS, (202) 338-6735,or write to P.O. Box 2604, Washington, D.C. 20013. Department of Defense consumers are required to submit requests through appropriate command validation channels to DIA, RTS-2C, Washington, D.C. 20301. (Telephone: (202) 373-3771, Autovon: 243-3771.)

Back issues or single copies of the DAILY REPORTs and JPRS publications are not available. Both the DAILY REPORTs and the JPRS publications are on file for public reference at the Library of Congress and at many Federal Depository Libraries. Reference copies may also be seen at many public and university libraries throughout the United States.